

Investigation of Lattice Effects in Perovskites by ^{18}O -isotope Exchange

Mitsuru Itoh*, Rajappan Mahesh and Ruiping Wang

Materials & Structures Laboratory Tokyo Institute of Technology 4259 Nagatsuta, Midori, Yokohama 226-8503, Japan
(Received September 23, 1998)

In the present study, preliminary experimental results of the change in the properties of perovskite-type oxides caused by the ^{18}O -exchange have been reported. Two systems were selected for the exchange, (1) ATiO_3 ($\text{A}=\text{Ca}, \text{Sr}, \text{Ba}$) and (2) manganese perovskite. The dielectric properties of isotope-exchanged $\text{SrTi}^{18}\text{O}_3$ showed a drastic change from a quantum paraelectricity below 3 K to ferroelectric-like behavior with a peak at 23 K and an enhanced dielectric constant, 35000 at the peak. On the contrary, the T_c for BaTiO_3 was found to increase by 0.9 K. The observed isotope shift of T_c as well as T_{∞} for the manganese perovskites is correlated with the key parameters controlling the lattice such as Mn^{3+} content, average ionic radius of the A-site cation $\langle r_A \rangle$ and A-site ionic disorder σ^2 .

Key words: Perovskite, Ferroelectricity, Isotope effect, Quantum effect, Disorder effect

I. Introduction

Investigation of the isotope effects on the properties of oxides have been an important subject of the solid state physics and chemistry since the change in the weight of the component atoms affects the frequency of phonons through the change in the reduced mass of the vibrating system of the relevant ions. The replacement of the isotopes of the ions have been carried out for many kinds of simple oxides and complex oxides, especially for the materials showing interesting properties such as cuprous superconductors, ferromagnetics, and ferroelectrics. In the present study, we have chosen two series of oxide materials for the isotope exchange, ATiO_3 ($\text{A}=\text{Ca}, \text{Sr}, \text{Ba}$) and manganese perovskite, AMnO_3 . CaTiO_3 and SrTiO_3 are known as quantum paraelectrics whose relative dielectric constant become constant below 20 and 3 K, respectively. On the contrary, BaTiO_3 is known to as ferroelectrics showing T_c at 410 K. Manganese perovskite is well known as GMR (Giant-Magneto-Resistance) materials.

1-1. ATiO_3 system

The dielectric constant of SrTiO_3 increases with decreasing temperature and attains a maximum as large as 20000 along its $\langle 001 \rangle$ direction.¹ After that the dielectric constant keeps that value down to 0.3 K.² This is qualitatively explained that the amplitude of the ferroelectric mode of the relevant mode becomes smaller than that of normal vibration of the ground state.² Other than SrTiO_3 , CaTiO_3 ,³ $\text{Ln}_{1/2}\text{Na}_{1/2}\text{TiO}_3$ ⁴⁻⁷ ($\text{Ln}=\text{La}, \text{Pr}, \text{Nd}, \text{Sm}, \text{Eu}, \text{Gd}, \text{Tb}, \text{Dy}, \text{Ho}, \text{Er}, \text{Lu}$) are known as quantum paraelectrics. Viewing these materials, SrTiO_3 is most interesting materials since it is in the critical regime between ferroelectrics and quantum paraelectrics.⁸ This critical situation is due to the critical

size of component ions, Sr, Ti, and O.⁹ At room temperature, tolerance factor for SrTiO_3 is 1.00, which means that SrTiO_3 possesses an ideal packing for perovskite. Viewing the perovskite structure SrTiO_3 from $\langle 100 \rangle$ direction, alternative stacking of SrO and TiO_2 can be seen. However, expansion coefficients in SrO and TiO_2 layers differ from each other and leads to a decrease in the tolerance factor at low temperatures, which is originating from the difference in the chemical bonds in these two layers, i.e., larger thermal expansion in the SrO layer with strong ionic character and relatively small thermal expansion in TiO_2 layer with stronger covalency. Therefore when the temperature is decreased, SrTiO_3 undergoes a phase transition from cubic $\text{Pm}\bar{3}\text{m}$ to tetragonal I4/mcm at 104 K. Relatively large thermal shrinkage in the rock salt SrO layer compresses the TiO_2 layer and yields tilting of TiO_6 octahedra with decreasing temperature.

At lower temperature, the dielectric constant of SrTiO_3 increases and finally attains a very large value of 20000 at 3 K then keeps the value down to 0.3 K.² This is caused by the competition of ferroelectric and paraelectric state. When the temperature decreases down to near 0 K, the phonon condensation occurs, that is, all the phonons fall into their ground states with the zero-point vibration. The relative amplitude of this zero-point vibration is larger than that of ferroelectric mode, yielding a constant dielectric constant at lower temperature range. This is the origin of the quantum paraelectricity. This critical state of SrTiO_3 at lower temperature is easily influenced by the external stress,⁸ electric field, and impurity.¹⁰ For example, uniaxial stress can turn the single crystalline SrTiO_3 into ferroelectric state and quite small amount of Ca^{2+} ion can cause a quantum ferroelectricity below 20 K.¹⁰ It is known that a large electric field results in a ferroelectric state with the small range in

the crystal.

1-2. Manganese perovskite

Rare earth manganates, AMnO_3 doped with bivalent ions such as Ca^{2+} , Sr^{2+} , Ba^{2+} at the A-site is known as early as 1950s and exhibit interesting electrical and magnetic properties.^{11),12)} Doping gives rise to mixed valence states of Mn^{3+} and Mn^{4+} introducing holes in the Mn-3d band. Manganates with optimal hole concentration or Mn^{4+} content undergoes paramagnetic insulator (PI) to ferromagnetic metal (FM)-like transition as the temperature decreases showing a peak in resistivity at a temperature, T_{I-M} close to the ferromagnetic Curie temperature (T_c). The simultaneous appearance of ferromagnetism and metal-like conductivity was explained by Zener introducing a novel double-exchange model. Accordingly, the conductivity arises due to the hopping of d-electron from the singly occupied $\text{Mn}^{3+} e_g$ orbital to the adjacent unoccupied $\text{Mn}^{4+} e_g$ orbital via intervening oxygen. The carriers preserve their spin orientation during hopping and are strongly coupled to the localized t_{2g} electron (Hund's Coupling, J) thereby stabilizing the ferromagnetic ground state. The transfer integral, t_{ij} of the carriers is sensitive to the angle between the adjacent t_{2g} spins (θ_{ij}) and is given by $t_{ij} = t_0 \cos(\theta_{ij}/2)$. Thus t_{ij} is maximized when $\theta_{ij} = 0$ or the Mn-O-Mn bond angle, ϕ ($\phi = 180 - \theta_{ij}$) is 180° . The J parameter enhances the magnetization dependence of resistivity below T_c .

The double exchange model based on t_{ij} and J however fails to account for the many observed properties including the insulating behavior in the paramagnetic regime above T_c and the recently observed colossal magnetoresistance in manganates. It is also intriguing that unlike the resistivity behavior below T_c , which is markedly affected by the A-site doping, the behavior above T_c is largely unaffected. Kusters *et al.*¹³⁾ have proposed the existence of magnetic polarons, charge carriers surrounded by magnetic polarization above T_c . De Teresa *et al.*¹⁴⁾ have later shown by volume thermal expansion, magnetic susceptibility and small angle neutron scattering experiments that magnetic polarons do exist above T_c . Millis *et al.*¹⁵⁾ have suggested that a polaron mechanism due to electron-phonon coupling originating from the dynamic Jahn-Teller (J-T) effect (which lifts the degeneracy of the e_g orbital of the Mn^{3+} ion) is essential to reduce the itinerant electron kinetic energy at T_{I-M} . The electron-phonon coupling constant, λ is directly proportional to the Jahn-Teller stabilization energy and is inversely proportional to the e_g electron transfer integral. Millis *et al.* have shown that the metal-insulator transition will occur when λ attains a critical value. A composite polaron consisting of magnetic and J-T polarons has also been proposed.¹⁶⁾

The prevalence of polaron in manganates is supported by a number of structural as well as non-structural evidences. The structural evidences come from the lattice distortion associated with the localized charge carriers. Billinge *et al.*¹⁷⁾ have found from their pair distribution function (PDF) analysis of the neutron powder diffraction data of $\text{La}_{1-x}\text{Ca}_x\text{MnO}_3$, a local structure change at T_{I-M} due to the isotro-

pic collapse of oxygen octahedron around Mn^{4+} . These authors have visualized the polarons as a breathing mode distortion of oxygen around manganese. The J-T distortion of the planar oxygen atoms leads to the separation of the neighboring Mn-O bonds by 0.1 \AA (above T_c), a value in agreement with the proposition of Millis *et al.* Louca *et al.*¹⁸⁾ have showed from the PDF study of neutron diffraction data on $\text{La}_{1-x}\text{Sr}_x\text{MnO}_3$ that J-T distortion is present locally in both insulating as well as metallic states and there is a direct correspondence between the J-T distortion and lattice polarons. Booth *et al.*¹⁹⁾ has observed unusual increase in Debye-Waller parameters of Mn-O and Mn-Mn atom pairs near T_c in $\text{La}_{1-x}\text{A}_x\text{MnO}_3$ ($A = \text{Ca}, \text{Pb}$) for compositions exhibiting I-M transition. The activated resistivity behavior above T_c and the relatively lower value of the activation energy of Hall coefficient compared with that of electrical conductivity provide non-structural evidences for the formation of polarons.^{20),21)}

The presence of polarons narrows down the effective band width (W_{eff}) according to the relation $W_{\text{eff}} \approx W \exp(-\gamma E_p/\hbar\omega)$ where E_p is the polaron stabilization energy and ω is the optical phonon frequency. ω depends on the lattice vibrations and is inversely proportional to the square root of the atomic mass. γ is a dimensionless factor and varies proportionately with E_p/W . In the strong coupling limit, where J exceeds W_{eff} it can be shown that $T_c \propto W_{\text{eff}}$. Thus, any perturbation in the lattice vibrations should affect T_c . This is demonstrated by Zhao *et al.*²²⁾ in the giant isotope shift of T_c ($T_c(^{16}\text{O}) - T_c(^{18}\text{O})$). T_c was found lowered by more than 20 K when ^{16}O is replaced with ^{18}O in $\text{La}_{0.8}\text{Ca}_{0.2}\text{MnO}_3$ while the effect was negligible in a similar ferromagnetic perovskite oxide SrRuO_3 with no J-T effect suggesting the presence of J-T polarons in the former. W_{eff} and hence T_c and related properties are also affected by the various factors responsible for lattice effects in manganates such as hydrostatic pressure, magnetic field, Mn^{4+} content, average ionic radius of the A-site cation ($\langle r_A \rangle$) and A-site ionic disorder (σ^2).²³⁾ The incorporation of ^{18}O in manganates therefore provides an effective means to systematically study the lattice effects. In this study, we have investigated a variety of normal as well as ^{18}O exchanged manganates exhibiting colossal magnetoresistance as well as charge ordering and tried to correlate the observed isotope shift with the Mn^{3+} content, $\langle r_A \rangle$ and σ^2 .

II. Results and Discussions

2-1. ATiO_3 system

Oxygen isotope exchange was conducted for single crystalline SrTiO_3 and CaTiO_3 and polycrystalline SrTiO_3 , CaTiO_3 , and BaTiO_3 . All the samples were heated in $^{18}\text{O}_2$ gas atmosphere at 1273 K until their weights attain constant values. The exchange rates for all the samples were confirmed to be larger than 90%. Fig. 1 shows the temperature dependence of the relative dielectric constant, ϵ_r , for polycrystalline SrTiO_3 and BaTiO_3 . It is clearly shown that ferroelectric-

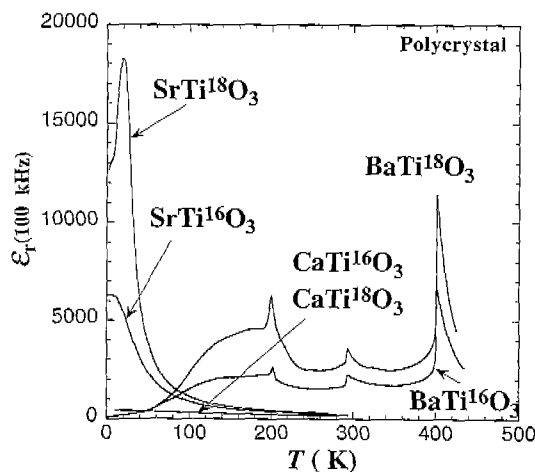


Fig. 1. Temperature dependence of relative dielectric constant for pristine and isotope exchanged CaTiO_3 , SrTiO_3 , BaTiO_3 .

like peak appears after the ^{18}O isotope exchange in SrTiO_3 . On the contrary, T_c increased by 0.9 K in BaTiO_3 . These results are intuitively well understood by considering the vibrational modes which are responsible for the ferroelectric transition. It is well known that Slater and Last modes are important for the evolution of ferroelectricity in the ferroelectrics with perovskite-type structure. We must emphasize that the almost equal atomic weights between the relevant atoms, Ti^{4+} and O_3^{2-} group, i.e., 47.94 for the former and $15.9994 \times 3 = 47.9982$ for the latter. When the ^{18}O is substituted for ^{16}O , the weight ratio turns to 47.94/54. The imbalance in the atomic weights of the atoms leads to an increase in the anharmonicity of vibrating system, yielding the evolution of ferroelectricity. The detail of the present work is to be reported elsewhere.²⁴⁾

2-2. Manganese perovskite system

2-2-1. Mn^{3+} content and giant oxygen isotope effect

The seminal role of Mn^{4+} content on the structure, magnetic and magnetoresistive properties of perovskite manganates has been clearly brought out by the investigations on undoped LaMnO_3 by Mahendiran *et al.*²⁵⁾ With increasing Mn^{4+} content LaMnO_3 undergoes structural transitions from orthorhombic \rightarrow rhombohedral \rightarrow pseudocubic. While rhombohedral as well as pseudocubic LaMnO_3 show higher T_c and magnetoresistance, orthorhombic phase with relatively lower Mn^{4+} content remains as antiferromagnetic insulator with very low magnetoresistance.

To explore the relationship between Mn^{3+} content (here we use Mn^{3+} instead of Mn^{4+} to highlight the J-T effect in the former) on the oxygen isotope effect we have investigated $\text{La}_{1-x}\text{Ca}_x\text{MnO}_3$ compositions with 'x' varying from 0.1-0.4. $\text{La}_{1-x}\text{Ca}_x\text{MnO}_3$ is an ideal system for such a study as La and Ca have nearly same ionic radius. This rules out the contributions from $\langle r_A \rangle$ and σ_2 . In addition the orthorhombic symmetry is retained in the entire range of solid solution.²⁶⁾ In a typical experiment we have four samples: the

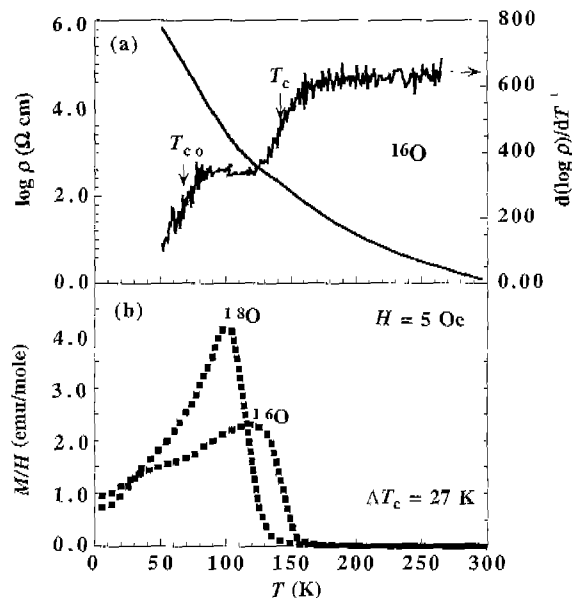


Fig. 2. Temperature dependence of (a) $\log \rho$ and $d \log \rho / dT^{-1}$ of $\text{La}_{0.9}\text{Ca}_{0.1}\text{MnO}_3$ (^{16}O) and (b) magnetic susceptibility of ^{16}O as well as ^{18}O $\text{La}_{0.9}\text{Ca}_{0.1}\text{MnO}_3$ samples.

as-prepared, ^{16}O heated, ^{18}O exchanged and $^{18}\text{O} \xrightarrow{\Delta} ^{16}\text{O}$ back-exchanged. The details of the sample preparation is described elsewhere.²⁷⁾ The average isotope exchange rate is $85 \pm 5\%$ and back-exchange rate is $90 \pm 5\%$ as determined from the weight change. Electrical resistivity measurements were carried out on various samples using the standard four probe method and magnetization measurements were done using a Quantum Design MPMS magnetometer. The magnetization data were recorded on warming after the samples were cooled to 5 K in zero field. The results of the back-exchanged samples have ensured the reversibility of the isotope exchange process.

In Fig. 2 (a) we show the temperature variation of resistivity of ^{16}O sample of $\text{La}_{0.9}\text{Ca}_{0.1}\text{MnO}_3$. The sample is insulating down to 50 K (the lowest temperature down to which measurements were carried out as the sample became more resistive). It can be seen from the $d \log \rho / dT^{-1}$ plot that this sample undergoes two successive transitions: (1) paramagnetic insulator \rightarrow ferromagnetic insulator around 145 K (2) ferromagnetic insulator \rightarrow charge ordered insulator around 70 K. The charge ordered state of this sample is very weak such that magnetic field as low as 100 Oe is just sufficient to melt it. Hence the measurements were carried out at a very low applied field of 5 Oe. In Fig. 2 (b) the magnetization data of ^{16}O and ^{18}O samples are given. The T_c of the ^{18}O sample is suppressed by 27 K. Zhou and Goodenough²⁸⁾ have shown that this remarkable suppression of T_c by ^{18}O substitution is due to the mass dependent trapping of mobile polarons above T_c . In Fig. 3 we plot the isotope shift of T_c as a function of Mn^{3+} content. The isotope shift of T_c increases monotonically with Mn^{3+} . It is to be noted that in $\text{La}_{1-x}\text{Ca}_x\text{MnO}_3$, T_c decreases with increasing Mn^{3+} content in the composition range under present study. As T_c increases

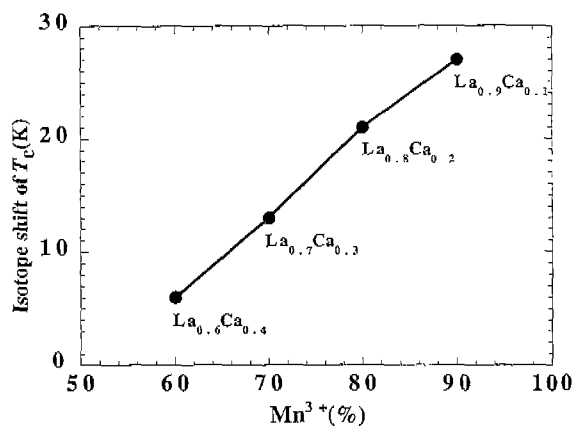


Fig. 3. Variation of the oxygen isotope shift of ferromagnetic Curie temperature, T_c with Mn^{3+} content.

the isotope shift of T_c decreases. A higher T_c corresponds to a higher W_{eff} , which in turn corresponds to weaker lattice-spin coupling. A larger isotope shift of T_c thus implies a stronger lattice-spin interaction. This could arise partly from the increase in magnitude of J-T effect with increasing Mn^{3+} content.

2-2-2. Critical role of $\langle r_A \rangle$

The Mn-O-Mn angle, ϕ and hence the e_g electron transfer integral, t_j , is markedly influenced by the size of the doping ion at the A-site.^{29,30} The Mn-O-Mn angle decreases with decreasing average ionic radius of the A-site cation ($\langle r_A \rangle$) resulting in the rotation of the MnO_6 octahedra to relieve the associated strain of the lattice. The effect of $\langle r_A \rangle$ on the properties of the manganates have been extensively reported in literature. Generally speaking, with decreasing $\langle r_A \rangle$, T_c decreases while resistivity and magnetoresistance increases dramatically. Thus, $\langle r_A \rangle$ provides an important chemically tunable parameter in manganates. Zhao *et al.*²² have shown that the oxygen isotope exponent α_o (defined as $-\ln T_c / \ln M$ where M is the mass of the oxygen isotope) increases drastically with decreasing $\langle r_A \rangle$. In other words, the isotope shift of T_c decreases with increasing $\langle r_A \rangle$ or larger e_g bandwidth.

Decreasing $\langle r_A \rangle$ in manganates suppresses ferromagnetism and enhances charge ordering instability. We have investigated the variation of the oxygen isotope shift of T_{∞} (charge ordering temperature) with $\langle r_A \rangle$. For this purpose, we have carried out isotope exchange in the well-known charge ordered manganates $Nd_{0.5}Sr_{0.5}MnO_3$, $La_{0.5}Ca_{0.5}MnO_3$ and $Pr_{0.5}Ca_{0.5}MnO_3$ having $\langle r_A \rangle$ of 1.236 Å, 1.198 Å and 1.179 Å respectively. In Fig. 4 we show the resistivity and magnetization data of ^{16}O , ^{18}O and back-exchanged ($^{18}O \rightarrow ^{16}O$) samples of $Nd_{0.5}Sr_{0.5}MnO_3$. The charge ordering transition temperature is enhanced by 21 K. It is to be noted that T_c did not show any appreciable change as expected of manganates with larger $\langle r_A \rangle$. The increment in T_{∞} could be due to the mass enhanced localization of charge carriers above T_{∞} . In the case of $Pr_{0.5}Ca_{0.5}MnO_3$ with very small $\langle r_A \rangle$ (see Fig. 5) the isotope shift of T_{∞} is negligibly small.

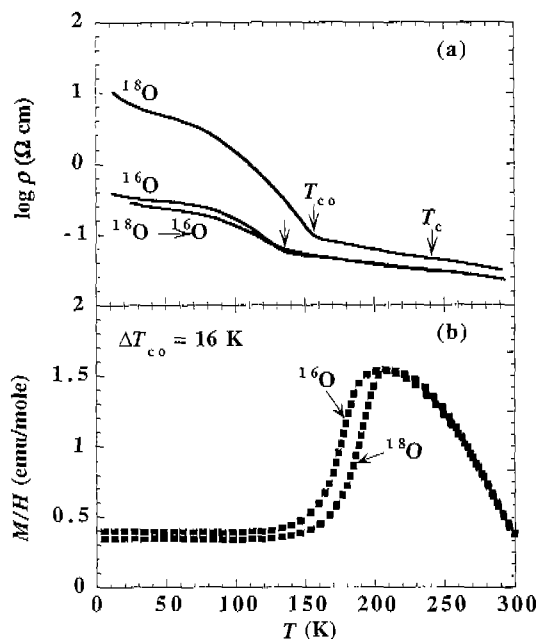


Fig. 4. Temperature dependence of (a) resistivity and (b) magnetic susceptibility of ^{16}O , ^{18}O and back-exchanged ($^{18}O \rightarrow ^{16}O$) samples of $Nd_{0.5}Sr_{0.5}MnO_3$.

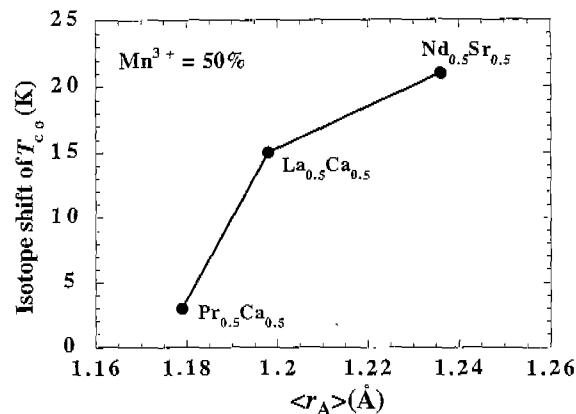


Fig. 5. Variation of oxygen isotope shift of charge ordering temperature, T_{∞} with the average ionic radius of the A-site cations $\langle r_A \rangle$.

This may be due to the unusual stability of the charge ordered state in the low $\langle r_A \rangle$ regime and the low mobility of carriers above T_{∞} . The isotope shift of T_{∞} is appreciable only in manganates with relatively large $\langle r_A \rangle$. At this point it is worth mentioning the report of Garcia-Landa *et al.*³¹ who have found that to melt charge ordering in $Pr_{2/3}Ca_{1/3}MnO_3$, a magnetic field of 12 T is required for ^{18}O sample instead of 6 T in the case of ^{16}O sample although there was no isotope shift of T_{∞} . The absence of isotope shift of transition temperature therefore does not necessarily mean the absence of isotope effect.

2-2-3. A-site disorder effects

Undoped rare earth manganates are antiferromagnetic

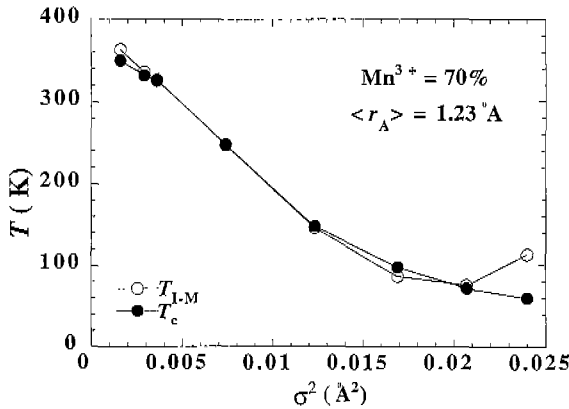


Fig. 6. Variation of T_c (T_{I-M}) with A-site disorder parameter, σ^2 for manganates with fixed Mn^{3+} content of 70% (adapted from Rodriguez-Martinez *et al.* 1996).

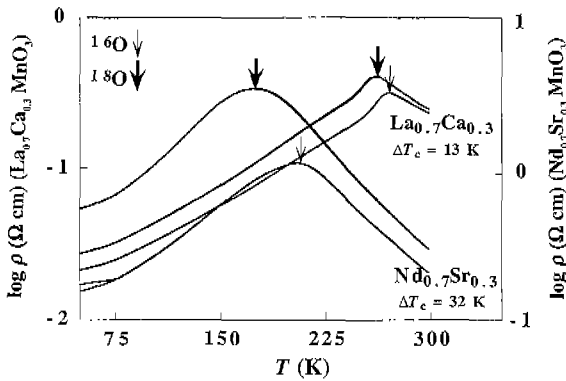


Fig. 7. Temperature dependence of resistivity of ^{16}O as well as ^{18}O samples of $\text{La}_{0.7}\text{Ca}_{0.3}\text{MnO}_3$ and $\text{Nd}_{0.7}\text{Sr}_{0.3}\text{MnO}_3$ showing the extent of the oxygen isotope shift.

insulators. The rich variety of fascinating properties of manganates known till to-date arises from doping. Doping by aliovalent ions at the A-site creates not only Mn mixed valency but also significant disorder at the A-site due to the differences in size of the rare earth and dopant ions. The manifestation of the disorder effects on the physical properties are primarily due to the displacement of oxygen atoms from their ideal crystallographic positions, the oxygen being an integral part of the Mn-O-Mn exchange interactions.

Rodriguez-Martinez and Paul Attfield³²⁾ have quantified the A-site disorder making use of the variance of the A-site cation radius distribution, σ^2 given by $\sum x_i r_i^2 - \langle r_A \rangle^2$ where x_i ($\sum x_i = 1$) represent the fractional occupancy of ion of radius r_i and $\langle r_A \rangle$ is the average ionic radius of the A-site cation described earlier. The variation of T_c and T_{I-M} for a number of manganates with fixed Mn^{4+} content of 30% and $\langle r_A \rangle$ of 1.23 \AA as obtained by these authors is given in Fig. 6. T_c as well as T_{I-M} decreases rather steeply with increasing σ^2 .

We have explored the effect of σ^2 on the isotope shift of T_c as well as T_{∞} . $\text{La}_{0.7}\text{Ca}_{0.3}\text{MnO}_3$ ($\langle r_A \rangle = 1.205 \text{ \AA}$; $\sigma^2 = 2.7 \times 10^{-4} \text{ \AA}^2$) and $\text{Nd}_{0.7}\text{Sr}_{0.3}\text{MnO}_3$ ($\langle r_A \rangle = 1.207 \text{ \AA}$; $\sigma^2 = 4.5 \times 10^{-3} \text{ \AA}^2$) with nearly same $\langle r_A \rangle$ and carrier concentration but with different σ^2 is subjected to isotope exchange. The resistivity data

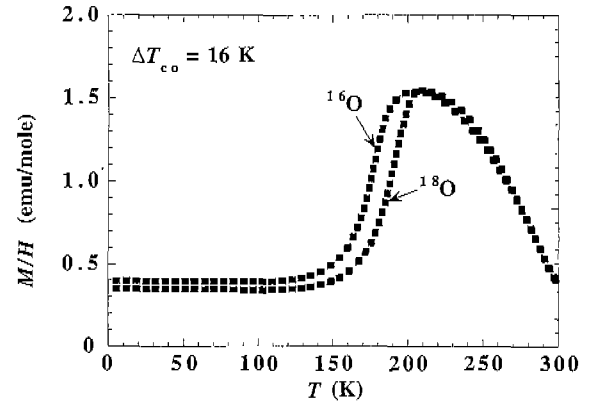


Fig. 8. Temperature dependence of magnetic susceptibility of ^{16}O and ^{18}O samples of $\text{La}_{0.5}(\text{Ca,Sr})_{0.5}\text{MnO}_3$.

of the ^{16}O and ^{18}O samples are shown in Fig. 7. $\text{La}_{0.7}\text{Ca}_{0.3}\text{MnO}_3$ with relatively smaller σ^2 shows higher T_c , but isotope shift of T_c (13 K) is smaller compared with $\text{Nd}_{0.7}\text{Sr}_{0.3}\text{MnO}_3$ which shows a lower T_c but larger shift of 32 K. A higher σ^2 implies a larger distortion of the lattice and stronger coupling. To investigate the effect of σ^2 on shift of T_{∞} we have carried out isotope exchange on $\text{La}_{0.5}(\text{Ca,Sr})_{0.5}\text{MnO}_3$ with $\langle r_A \rangle$ (1.236 \AA) same as that of the well-known charge ordered manganate $\text{Nd}_{0.5}\text{Sr}_{0.5}\text{MnO}_3$. The σ^2 for the former is $2.4 \times 10^{-3} \text{ \AA}^2$ and $5.4 \times 10^{-3} \text{ \AA}^2$ for the latter. $\text{La}_{0.5}(\text{Ca,Sr})_{0.5}\text{MnO}_3$ with smaller σ^2 shows (see Fig. 8) smaller isotope shift of T_{∞} of 16 K against 21 K (Fig. 4) for $\text{Nd}_{0.5}\text{Sr}_{0.5}\text{MnO}_3$.

III. Conclusions

Substitution of ^{18}O for ^{16}O in SrTiO_3 yielded a ferroelectric phase transition, which is caused by the enhancement of unharmonicity in the vibration of optical mode. The oxygen isotope shift of T_c and T_{∞} in perovskite manganates shows systematic dependence on the Mn^{3+} content, $\langle r_A \rangle$ and σ^2 and hence provide an insitu probe to study the lattice-spin coupling. Isotope shift of T_c increases with the content of the Jahn-Teller active Mn^{3+} ion. For fixed Mn^{3+} content and $\langle r_A \rangle$, enhanced shift of T_c is observed with increasing σ^2 . We find that the isotope shift of T_{∞} increases with $\langle r_A \rangle$. For given Mn^{3+} content and $\langle r_A \rangle$ increased isotope shift of T_{∞} is found with increasing σ^2 . Both isotope shifts of T_c as well as T_{∞} is observed in the intermediate range of $\langle r_A \rangle$. Isotope shift is negligible for manganates with very large $\langle r_A \rangle$ (wide band) as well as very small $\langle r_A \rangle$ (narrow band).

Acknowledgment

The authors wish to express their thanks to financial supports from Grant-in-Aid for Scientific Research from Ministry of Education, Science, Culture and Sports, JSPS Research Future Program, "ATOMIC-Scale Surface and INTERFACE DYNAMICS," Iketani Science and Technology Foundation, and The Sumitomo Foundation.

References

1. J. H. Barrett, "Dielectric Constant in Perovskite-Type Crystals," *Phys. Rev.*, **86**, 118 (1952).
2. K. A. Muller and H. Burkard, "SrTiO₃: An Intrinsic Quantum Paraelectric Below 4 K," *Phys. Rev. B*, **19**, 3593 (1979).
3. I.-S. Kim, M. Itoh and T. Nakamura, "Electrical Conductivity and Metal-Nonmetal Transition in the Perovskite-Related Layered System Ca_{n+1}Ti_nO_{3n+1.3} (n=2,3 and ∞)," *J. Solid State Chem.*, **101**, 77 (1992).
4. Y. Inaguma, J. H. Sohn, I.-S. Kim, M. Itoh and T. Nakamura, "Quantum Paraelectricity in a Perovskite La_{1/2}Na_{1/2}TiO₃," *J. Phys. Soc. Jpn.*, **61**, 3831 (1992).
5. P. H. Sun, T. Nakamura, Y.-J. Shan, Y. Inaguma and M. Itoh, "High Temperature Quantum Paraelectricity in Perovskite-type La_{1/2}Na_{1/2}TiO₃ (Ln=Pr, Ne, Sm, Eu, Gd and Tb)," *Ferroelectrics*, **200**, 93 (1997).
6. Y.-J. Shan, T. Nakamura, Y. Inaguma and M. Itoh, "Preparation and Dielectric Characterization of the Novel Perovskite-type Oxides La_{1/2}Na_{1/2}TiO₃ (Ln=Dy, Ho, Er, Tm, Yb, Lu)," *Solid State Ionics*, **108**, 123 (1998).
7. T. Nakamura, Y.-J. Shan, P.-H. Sun, Y. Inaguma and M. Itoh, "The Cause of the High Temperature Quantum Paraelectricity in Some Perovskite Titanate," *Solid State Ionics*, **108**, 53 (1998).
8. H. Uwe and T. Sakudo, "Stress-induced Ferroelectricity and Soft Phonon Modes in SrTiO₃," **13**, 271 (1976).
9. R. D. Shannon, "Revised Effective Ionic Radii and Systematic Studies of Interatomic Distances in Halides and Chalcogenides," *Acta Cryst.*, **A32**, 751 (1976).
10. J. G. Bednortz and K. A. Müller, "Sr_{1-x}Ca_xTiO₃: An XY Quantum Ferroelectric with Transition to Randomness," *Phys. Rev. Lett.*, **52**, 2289 (1984).
11. G. H. Jonker and J. H. Van Santen, "Ferromagnetic Compounds of Manganese with Perovskite Structure," *Physica (Utrecht)* **16**, 337 (1950).
12. E. O. Wollan and W. C. Koehler, "Neutron Diffraction Study of the Magnetic Properties of the Series of Perovskite-type Compounds [(1-x)La, xCa]MnO₃," *Phys. Rev.*, **100**, 545 (1955).
13. R. M. Kusters, J. Singleton, D. A. Keen, R. McGreevy and W. Hayes, "Magnetoresistance Measurements of the Magnetic Semiconductor Nd_{0.5}Pb_{0.5}MnO₃," *Physica (Amsterdam)*, **155B**, 362 (1989).
14. J. M. De Teresa, M. R. Ibarra, P. A. Algarabel, C. Ritter, C. Marquina, J. Blasco, J. Garcia, A. del Moral and Z. Arnold, "Evidence for Magnetic Polarons in the Magnetoresistive Perovskites," *Nature*, **386**, 256 (1997).
15. A. J. Millis, P. B. Littlewood and B. I. Shraiman, "Spiral State and Giant Magnetoresistance in Perovskite Mn Oxides," *Phys. Rev. Lett.*, **74**, 3407 (1995).
16. L. J. Zou, H. Q. Lin and Q. Q. Zheng, "Tunneling Evidence of Half-metallicity in Epitaxial Films of Ferromagnetic Perovskite Manganites and Ferrimagnetic Manganite," *J. Appl. Phys.*, **83**, 7363 (1998).
17. S. J. L. Billinge, R. G. DiFrancesco, G. H. Kwei, J. J. Neumeier and J. D. Thompson, "Direct Observation of Lattice Polaron Formation in the Local Structure of La_{1-x}Ca_xMnO₃," *Phys. Rev. Lett.*, **77**, 715 (1996).
18. D. Louca, T. Egami, E. L. Brousha, H. Roder and A. R. Bishop, "Local Jahn-Teller distortion in La_{1-x}Sr_xMnO₃ Observed by Pulsed Neutron Diffraction," *Phys. Rev. B*, **56**, 8475 (1997).
19. C. H. Booth, F. Bridges, S. J. Snyder and T. H. Geballe, "Evidence of Magnetization-dependent Polaron Distribution in La_{1-x}A_xMnO₃, A=Ca, Pb," *Phys. Rev. B*, **54**, R15606 (1996).
20. G. J. Snyder, R. Hiskes, S. DiCarolis, M. R. Beasley and T. H. Geballe, "Intrinsic Electrical Transport and Magnetic Properties of La_{0.67}Ca_{0.33}MnO₃ and La_{0.67}Sr_{0.33}MnO₃ MOCVP Thin Films and Bulk material," *Phys. Rev. B*, **53**, 14434 (1996).
21. M. Jaime, H. T. Hardner, M. B. Salamon, M. Rubinstein, P. Dorsey and D. Emin, "Hall-Effect Sign Anomaly and Small-Polaron Conduction in (La_{1-x}Gd_x)_{0.67}Ca_{0.33}MnO₃," *Phys. Rev. Lett.*, **78**, 951 (1997).
22. G. M. Zhao, K. Conder, H. Keller and K. A. Muller, "Giant Oxygen Isotope Shift in the Magnetoresistive Perovskite La_{1-x}Ca_xMnO_{3+y}," *Nature (London)*, **381**, 676 (1996).
23. C. N. R. Rao, A. K. Cheetham and R. Mahesh, "Giant Magnetoresistance in Transition Metal Oxides," *Chem. Mater.*, **8**, 2421 (1996).
24. M. Itoh *et al.*, unpublished work.
25. R. Mahendiran, S. K. Tiwari, A. K. Raychaudhuri, T. V. Ramakrishnan, R. Mahesh, N. Rangavittal and C. N. R. Rao, "Structure, Electron-transport Properties, and Giant Magnetoresistance of Hole-doped LaMnO₃ System," *Phys. Rev. B*, **53**, 3348 (1996).
26. S. W. Cheong and H. Y. Hwang, *Colossal Magnetoresistance Oxides* ed. Y. Tokura, Gordon & Breach, Monographs in Condensed Matter Physics.
27. R. Mahesh and M. Itoh, (to be published).
28. J. S. Zhou and J. B. Goodenough, "Phonon-Assisted Double Exchange in Perovskite Manganites," *Phys. Rev. Lett.*, **80**, 2665 (1998).
29. R. Mahesh, R. Mahendiran, A. K. Raychaudhuri and C. N. R. R. Ao, "Giant Oxygen Isotope Shift in the Magnetoresistive Perovskite La_{1-x}Ca_xMnO_{3+y}," *J. Solid State Chem.*, **120**, 204 (1995).
30. H. Y. Hwang, S. W. Cheong, P. G. Radaelli, M. Marezio and B. Batlogg, "Lattice Effects on the Magnetoresistance in Doped LaMnO₃," *Phys. Rev. Lett.*, **75**, 914 (1995).
31. B. Garcia-Landa, M. R. Ibarra, J. M. De Teresa, G. M. Zhao, K. Conder and H. Keller "Oxygen-Isotope Effect on the Field-Induced Metal-Insulator Transition in Pr_{2/3}Ca_{1/3}MnO₃," *Solid State Commun.*, **105**, 567 (1998).
32. L. M. Rodriguez-Martinez and J. P. Attfield, "Cation Disorder and Size Effects in Magnetoresistive Manganese Oxide Perovskites," *Phys. Rev. B*, **54**, R15622 (1996).